SPLIT-FEED CIRCUIT DESIGN FOR PRIMARY SULFIDE RECOVERY

*Michael J. Mankosa[1], Jaisen N. Kohmuench[1], Gerald H. Luttrell[2], John A. Herbst[3] and Aaron Noble[3]

[1]Eriez Flotation Division
2200 Asbury Road
Erie, Pennsylvania USA 16506
*(*Corresponding author: mmankosa@eriez.com)*

[2]Department of Mining & Minerals Engineering
100 Holden Hall, Virginia Tech
Blacksburg, Virginia USA 24061

[3]Department of Mining Engineering
365A Mineral Resources Building, West Virginia University
Morgantown, West Virginia USA 26506

ABSTRACT

The HydroFloat™ is an innovative fluidized-bed separator that can substantially increase the upper particle size that can be successfully treated by flotation. Recent studies conducted using laboratory, bench-scale and pilot-scale equipment indicate that this technology can be used to float coarse sulfide middlings that cannot be recovered by conventional flotation machines. Recent data collected from pilot-scale tests conducted at a base metal concentrator indicate that this technology can float middlings particles as large as 850 microns in diameter containing as little as 1% exposed hydrophobic mineral. As such, the crossover of this technology into the base metals industry has the potential to substantially reduce grinding costs and increase concentrator recovery/capacity through the use of split-feed circuitry. The split-feed concept, which is often used for upgrading industrial minerals, involves segregation of the feed into more than one size class followed by subsequent upgrading using mills/separators/reagents specifically optimized for each size class. In this article, a split-feed circuit is described that utilizes two stages of classifying cyclones in conjunction with the HydroFloat™ separator. The circuit is designed to recover, recycle and regrind coarse middlings containing small amounts of valuable mineral while simultaneously rejecting coarse well-liberated siliceous gangue so that mill throughput can be increased. Simulation data conducted using well-known process models suggest that this approach can increase existing primary mill capacity by up to 25% with only modest investments in new classifying and flotation equipment.

KEYWORDS

Circuit Design, Circuit Simulation, Split-Feed Flotation, Coarse Particle Flotation

INTRODUCTION

Froth flotation is often cited as one of the most important technological developments of the early 19th century. Without flotation technology, most of the raw materials required to sustain the world's energy, construction and manufacturing industries would be too costly to recover from the global resources of low-grade mineral deposits. Unfortunately, the effectiveness of this otherwise robust process is limited to a relatively narrow range of particle sizes. For the case of sulfide minerals, this critical range is limited to a narrow band of particle diameters between about 10 and 100 microns. This limitation is well illustrated by the size-by-size flotation data reported by Lynch et al. (1981) for industrial flotation plants operating in the base-sulfide industry (Figure 1). The addition to this plot of new size-by-size recovery data from recent audits of modern flotation plants shows that little has changed in the past several decades to expand the size range of applicability of froth flotation for upgrading sulfide minerals.

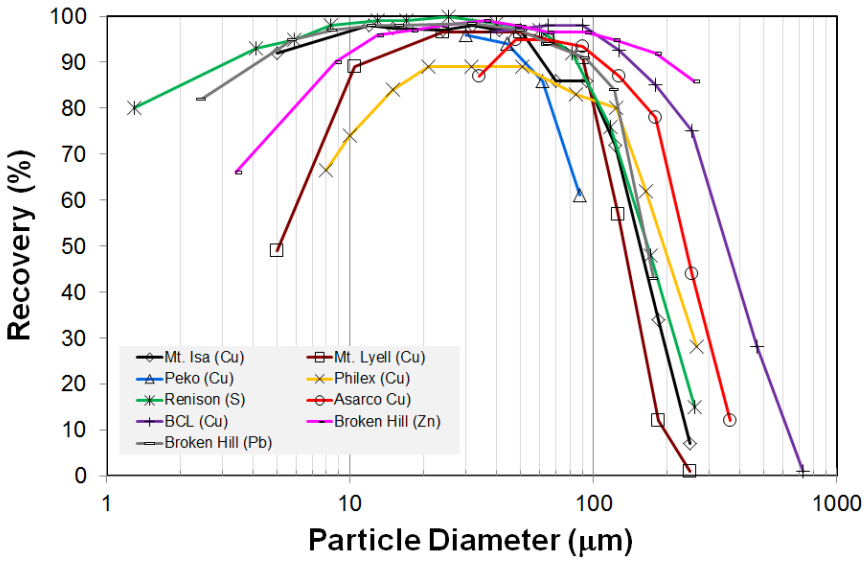

Figure 1 – Conventional flotation data for industrial sulfide flotation circuits (Lynch et al., 1981).

The underlying mechanisms responsible for the decline in flotation recovery of very fine and very coarse particles have been extensively discussed in the technical literature. The poor recovery of particles finer than about 10 microns has been historically attributed to the low hydrodynamic collision frequency between very small micron-size particles and relatively large millimeter-size bubbles (Trahar and Warren, 1976). Fines flotation can also be challenging due to the high particle surface area-to-mass ratio that can overload the bubble carrying capacity of industrial flotation systems (Yianatos et al., 1988) and adversely impact the surface chemical interactions that are necessary for effective collector coverage (Laskowski, 1989). For very coarse particles, the decline in recovery has been attributed to several longstanding problems such as poor mineral surface exposure (Schultz, 1977), increased bubble-particle detachment (Scheludko et al., 1976), reduced aggregate buoyancy (Schultz, 1984) and bubble overloading (King et al., 1974). These phenomena, which have been recognized for more than eight decades (Gaudin et al., 1931), can severely limit the recovery of coarse sulfide minerals in industrial flotation systems.

HYDROFLOAT™ TECHNOLOGY

In 2001, engineers at the Eriez Flotation Division (EFD) introduced an entirely new generation of flotation equipment to the minerals processing industry (Mankosa and Luttrell, 2001). This unique technology, which is currently marketed under the tradename HydroFloat™, was specifically developed to address and overcome the longstanding shortcomings of conventional machine designs in floating very coarse particles. The machine has already made tremendous impacts in several sectors of the industrial

minerals market for the collection of very coarse particles that were once believed to be unrecoverable by froth flotation technology. As such, this technology is now a standard unit operation in many potash and phosphate concentrators where grain sizes exceeding 0.5 mm are commonly floated.

As shown in Figure 2, the HydroFloat™ separator consists of an open tank subdivided into three sections. During operation, deslimed feed slurry is introduced into the upper section of the tank. At the same time, a regulated flow of process water is added just above the bottom section of the tank though an engineered network of distribution pipes. The upward flow of water creates a dense fluidized bed of suspended particles consisting primarily of non-floating (tailing) solids. Flotation is created by passing the fluidization water through an external high-shear bubble generator where a low flow of compressed gas and small dosage of frother is added just before the gas-water mixture is introduced into the distribution network. Finely dispersed bubbles generated by the sparging system are carried by the water into the fluidized bed where they are efficiently forced into contact with the densely-packed particles. Upon attachment to hydrophobic particles, the resulting bubble-particle aggregates are carried by the upward rising flow of fluidization water into the overflow launder. Hydrophilic solids continue to pass through the fluidized bed and accumulate in the lower dewatering cone located below the water distribution network. A control valve is used to regulate the discharge of underflow solids in response to one or more density readings from pressure transmitters placed within the fluidized bed.

Because of the unique design features, the HydroFloat™ separator offers several important advantages for treating coarser feed streams including reduced turbulence, improved bubble-particle contacting, minimization of buoyancy restrictions, elimination of froth-pulp transfer limitations, increased particle residence time, and plug-flow separating conditions (Mankosa and Luttrell, 2003). The machine also has no internal moving wear parts other than the pumping system, thereby greatly simplifying equipment maintenance. While these unique aspects of the HydroFloat™ separator have been described in detail by Kohmuench et al. (2010), several of the most important of these are discussed below.

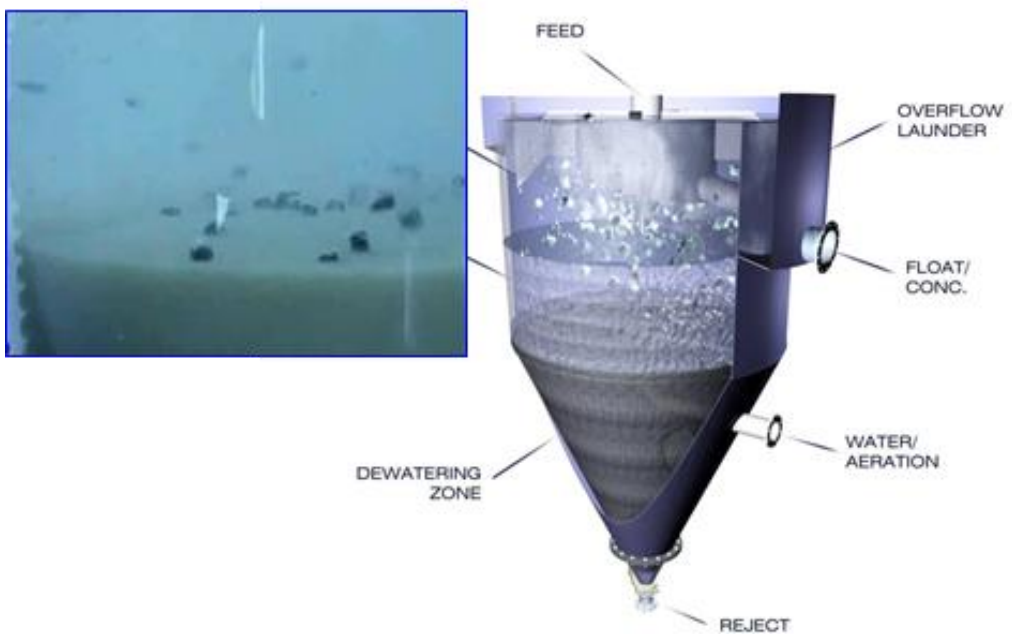

Figure 2 – Simplified schematic of the HydroFloat™ separator.

Bubble-Particle Buoyancy

One of the most obvious problems addressed by the HydroFloat™ technology is the issue of bubble-particle buoyancy. For spherical particles, a static force balance can be used to derive an expression for the maximum diameter (D_{max}) of a single bubble-particle aggregate that can rise in water (Schulze, 1984), i.e.:

$$D_{\max} = D_b \left(\frac{\rho_p - \rho_f}{\rho_f} \right)^{1/3} \quad (1)$$

where D_b is the bubble diameter, ρ_p is the particle density and ρ_f is the fluid density. This equation is plotted in Figure 3 as a function of particle density for a bubble diameter of 1 mm rising in water (ρ_f=1 gm/cm^3). This line shows that the maximum size of particles that can be floated under free-rise conditions in water declines sharply as the density of the particle increases. For example, Eq. (1) shows that a particle of pure chalcopyrite (ρ_p=4.2 gm/cm^3) would need to be smaller than 678 microns in diameter in order to be sufficiently buoyant to be floated in pure water.

Two additional cases need to be considered in the buoyancy calculations. The first is whether the bubble-particle aggregate can rise upward through the froth phase. As shown in Figure 4, the lower density of the froth phase can create a barrier to the recovery of coarse particles. The photograph shows a large bubble-covered particle that has sufficient buoyancy to float to the top of the water/pulp phase, but too little buoyancy to transfer up and through of the froth phase. The lower curve plotted in Figure 3 effectively illustrates this impact of this phenomenon for a case in which the froth density at the base is assumed to be 90% gas by volume (ρ_f=0.1 gm/cm^3). As expected, the maximum size that can rise through this low-density phase is greatly reduced even for low-density particles. For the case of chalcopyrite (ρ_p=4.2 gm/cm^3), the froth transfer limitation would theoretically only allow particles smaller than 290 microns to be recovered using 1 mm bubbles. The attachment of multiple bubbles to the particle can help

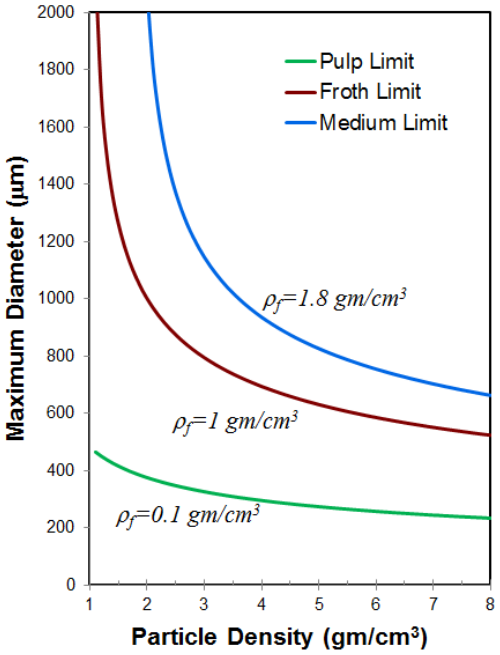

Figure 3 – Maximum particle diameter that can be buoyed in phases of different apparent densities based on Eq. [1]. (D_b=1 mm).

Figure 4 – Coarse particle trapped below the froth phase in a micro-flotation cell due to inadequate buoyancy of the particle-bubble cluster.

minimize this problem, although this is difficult for coarse poorly liberated solids that may have only a small patch of exposed mineral surface available for bubble attachments. In the HydroFloat™ unit, this limitation is completely eliminated since the machine operates in overflow mode without a froth-pulp transfer restriction.

The final buoyancy condition that needs to be considered for the HydroFloat™ separator is the effect of the high-density fluidized bed on the retention of bubble-particle aggregates. The upper line in Figure 3 shows how the projected maximum floatable particle size increases as the apparent fluid density is changed from water (ρ_f=1 gm/cm^3) to a packed-bed of fluidized solids (ρ_f=1.8 gm/cm^3). For 1 mm diameter bubbles, this effect shifts the D_{max} from 678 to 909 microns for the case of floating pure chalcopyrite (ρ_p=4.2 gm/cm^3). In practice, the attachment of even a single bubble to a hydrophobic particle lowers the net density of the resulting bubble-particle aggregate to a value that is lower than that of the fluidized bed. As such, the bubble-particle aggregate remains on the upper surface of the fluidized bed until a sufficient volume of bubbles attach to the particle to buoy it upward through the top section of the tank and into the overflow launder. For cases involving large amounts of hydrophobic solids, recovery can also be enhanced through the formation of multiple bubble-particle clusters that are created when single bubble-particle aggregates combine with other bubbles and particles to form clusters. While literature studies indicate that these clusters can improve the recovery of coarse particles (Ata et al., 2009; Drzymala, 1994a), it should be noted that experimental studies by the authors indicate that these clusters often require the upward flow of fluidization water in order to be hydraulically lifted upward into the overflow launder.

While the buoyancy analyses have been greatly simplified for brevity sake, it should be apparent that the intentional elimination of the froth phase and the creation of a fluidized bed of solids make it possible for the HydroFloat™ technology to recover much larger particles than can be achieved using traditional froth flotation machines. This suggestion is supported by laboratory experiments conducted by Dryzmala (1994b), which confirmed that coarse particles several millimeters in diameter can be readily floated in "frothless" Hallimond tube tests (stream of single bubbles with no froth phase) provided that the particles were adequately hydrophobic.

Bubble-Particle Contacting

One of the unique characteristics of the HydroFloat™ separator is how bubbles and particles are brought into contact within the aerated fluidized bed of solids. The hindered settling/rise condition within the fluidized bed substantially reduces the differential velocity between bubbles and particles, which in turn increase the contact time and likelihood of successful adhesion between bubbles and hydrophobic particles. The high solids concentration within the teeter bed also improves the attachment rate by increasing the collision frequency between bubbles and particles. This phenomenon occurs due to the compression of the fluid streamlines around the bubbles as they rise through the teeter bed. The increased probability of collision results in reaction rates that are several orders of magnitude higher than that found in conventional flotation machines. The high solids content of the fluidized bed also increases the particle residence time by decoupling the flow of solids from the flow of liquid. In most flotation processes, feed particles move with the fluid flow towards the discharge point in a co-current action. In contrast, particles move in the opposite direction to the fluid flow in the HydroFloat™ system. This counter-current action has obvious advantages since the effective settling velocity of the particles is reduced by the upward flow of fluidization water. In addition, the hindered settling conditions within the teeter bed never allow the particles to achieve their terminal free-fall velocity. Therefore, the fluidization water provides a significant increase in the particle retention time. The longer retention time allows good recoveries to be maintained without increasing cell volume. The HydroFloat™ also operates under nearly plug-flow conditions because of the low degree of axial mixing afforded by the uniform distribution of particles across the teeter bed. Consequently, the cell operates as if it were comprised of a large number of cells in series. Provided that all other conditions are equal, this characteristic allows a single unit to achieve the same recovery as a multi-cell bank of conventional cells. In other words, the HydroFloat™ separator makes more effective use of the available cell volume than well-mixed conventional cells or open columns.

Another advantage of the aerated fluidized bed used by the HydroFloat™ technology is the low degree of pulp turbulence. Interestingly, recent studies by Gontijo et al. (2007) have suggested that pulp turbulence has little impact on coarse particle flotation since a similar upper size limit was observed in their flotation experiments with quiescent column cells and agitated mechanical machines. However, this finding appears to contradict other literature reports suggesting that low turbulence is often beneficial for coarse particle flotation. For example, Barbery (1984) stated that the optimum conditions for coarse particle flotation occur when cell agitation intensity is reduced to a point just sufficient to maintain the particles in suspension. This study concluded that the maximum size of particles that can be recovered by flotation increases by more than an order of magnitude when changing from highly turbulent to quiescent conditions. Several other studies have shown that the maximum floatable particle size drops dramatically when conditions are turbulent, but can increase to more than several millimeters when conditions are quiescent (Woodburn et al., 1971; King & Colborn, 1971). The use of a fluidized bed in the HydroFloat™ separator makes it possible to keep particles dispersed and in suspension without the intense agitation required by mechanical flotation machines. As such, the low turbulence within the HydroFloat™ separator is ideal hydrodynamic environment for maximizing bubble-particle contacting while minimizing unwanted particle detachment.

SPLIT-FEED FLOTATION CIRCUITS

Recent experimental studies have shown that the HydroFloat™ technology can successfully float coarse low-grade middlings that are currently lost in industrial flotation circuits (Kohmuench et al., 2013; Mankosa et al., 2016). Moreover, advanced 3D-CT liberation studies by Miller et al. (2016) indicate that mineral grains as coarse as 850 microns and containing as little as 1% exposed sulfide mineral can be recovered using the HydroFloat™ technology in scavenging applications. This unique capability provides a new opportunity for the sulfide mineral industry to improve the capacity and lower the costs of their existing plant operations.

One particularly exciting retrofit configuration is to use the HydroFloat™ technology to reject well-liberated siliceous gangue from primary grinding circuits at a relatively coarse size, thereby making room for new feed tonnage in the primary grinding circuit. For example, consider the hypothetical base-sulfide flowsheet shown in Figure 5(a). This simplified flowsheet includes a primary grinding mill, primary classifying cyclones, rougher-scavenger flotation banks, cleaner flotation columns and a middlings regrind mill. The availability of the HydroFloat™ technology allows the circuit to be modified as shown in Figure 5(b). In this case, the primary classifying cyclones are reconfigured to provide a substantially coarser size cut (e.g., D_{80} increased from 200 to 300 microns). This layout allows the underflow to be passed back to the primary mill, while the overflow is passed to a secondary set of classifying cyclones. The secondary cyclone bank produces a fine (e.g., minus 200 micron) overflow that is sufficiently liberated to be

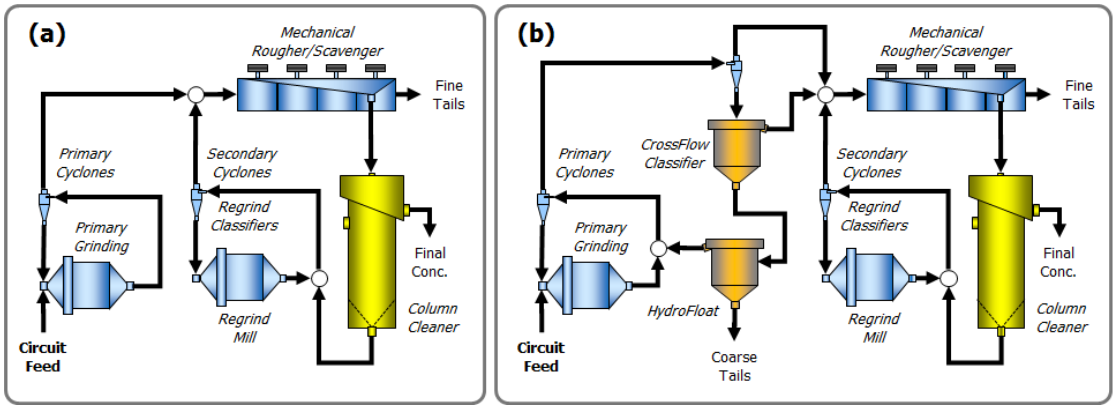

Figure 5 – Examples of (a) the simplified baseline flowsheet and (b) modified split-feed flowsheet incorporating the HydroFloat™ technology.

upgraded by the downstream conventional/column flotation circuit and a coarse (e.g., nominal 200 x 300 micron) underflow that is passed to the HydroFloat™ circuit. In this case, feed to the HydroFloat™ is reclassified using a CrossFlow separator to ensure near-complete removal of fines. The HydroFloat™ is then used as a highly efficient scavenger to ensure that all particles containing valuable sulfide mineral report to the overflow concentrate, which is recycled back to the primary grinding mill for further size reduction and liberation. The HydroFloat™ underflow, which consists of coarse liberated gangue, is rejected as a throw-away product that is essentially free of valuable mineral. As such, the siliceous gangue tonnage rejected by the HydroFloat™ makes room for new feed tonnage in the primary grinding mill. It is very important to note that the proposed HydroFloat™ circuit in not "flash flotation" as has been advocated in the past. Flash flotation attempts to remove liberated sulfide minerals that are trapped in the classifying circuit of a primary grinding mill due to their higher density. While this prevents over-grinding of the sulfide minerals, this does little to improve mill capacity. In contrast, the proposed HydroFloat™ circuit is designed to reject large tonnages of well-liberated siliceous gangue that often consumes a large volume of the circulating load in primary grind circuits. The replacement of coarse circulating gangue with new fresh feed provides an opportunity for the proposed circuit to dramatically increase concentrator capacity with only modest investments in new equipment for classification and flotation.

CIRCUIT SIMULATIONS

Modeling Approach

To demonstrate the advantages of split-feed circuitry, a hypothetical case study was undertaken in which the impact of the HydroFloat™ technology on grinding mill performance was investigated using a series of mathematical simulations. These simulations were done with Population Balance Models (PBMs) using ore characteristics representative of a typical copper porphyry ore. A 13-size fraction model was used throughout with 3 components (free valuable, locked middlings and free gangue**)** as described by Herbst et al. (1988). The feed size distribution (Figure 6) shows a moderately coarse feed, with an 80% feed passing size (F_{80}) of approximately 1.2 mm. Liberation between the classes was modeled using a size-by-size liberation model for typical porphyry copper ore. The feed ore was assumed to have a constant circuit feed grade of 0.58% Cu. Selection and breakage functions were chosen to mimic the Bond-specified Work Index of porphyry copper ore equal to 13.3 kWh/t. The specific selection function used in the simulation routine is shown in Figure 7. The partition models for the classifying cyclones (Figure 8) and CrossFlow classifier (Figure 9) were of the Nageswarorao (1995) type modified for the three specific gravities associated with each of the components. A variation on a teeter bed structure was used as a basis for the HydroFloat™ PBM (Figure 10). Data for this model was obtained from extensive laboratory and pilot-scale testing programs of porphyry copper ores carried out during the past five years. Lastly, a rougher

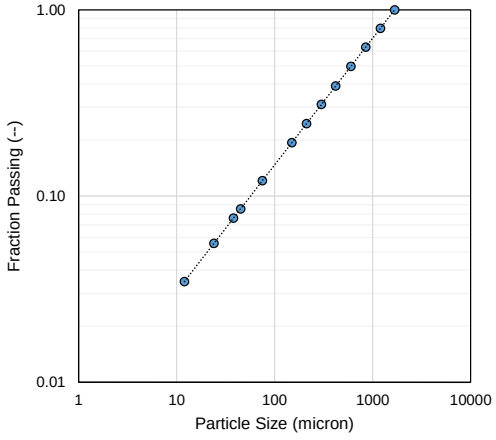

Figure 6 – Feed size distribution for typical porphyry copper ore used in the simulations.

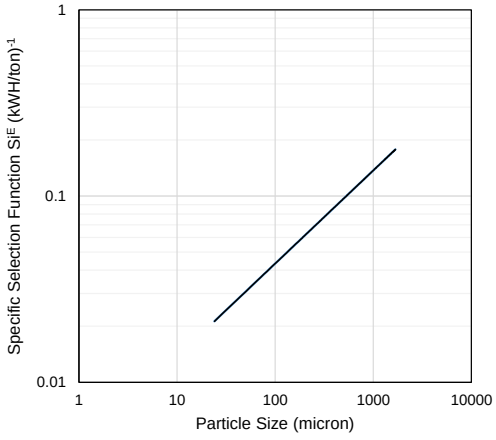

Figure 7 – Specific selection function for typical porphyry copper ore used in the simulations.

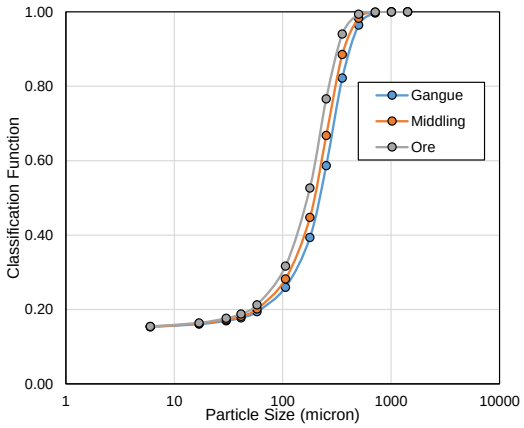

Figure 8 – Separation curves for primary cyclones.

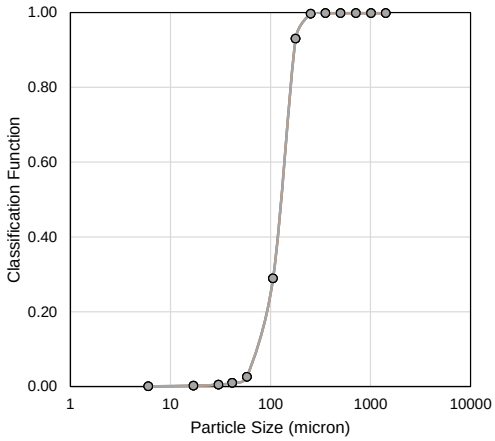

Figure 9 – Separation curve for CrossFlow

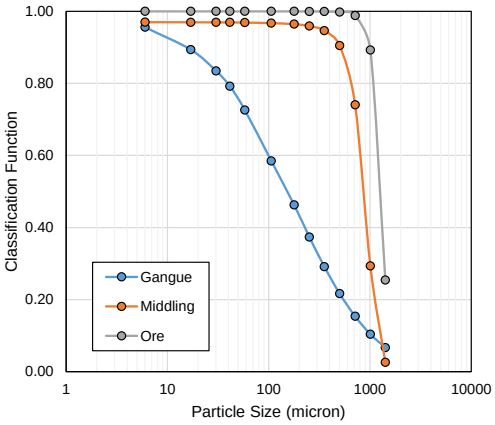

Figure 10 – Size-by-size recovery for simulation of HydroFloat™ separator.

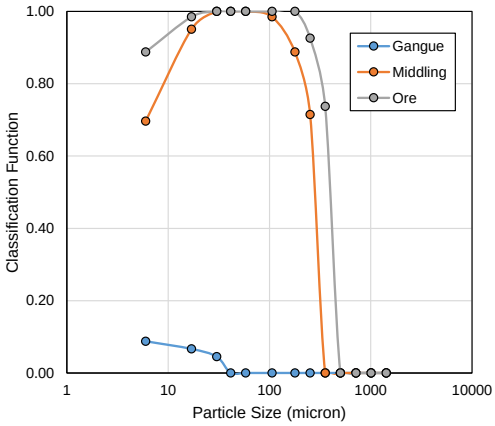

Figure 11 – Size-by-size recovery for simulation of rougher flotation.

flotation model was based on the cells-in-series, perfectly mixed reactor model, with size-by-component kinetic coefficients. Figure 11 shows recovery as a function of particle size for the three components. This recovery model closely matches the general size-by-size flotation trend shown earlier in Figure 1. Since the intent of the circuit simulation is to investigate primary grinding circuit performance, downstream units, including cleaner flotation and regrinding, were not considered in this study and will be addressed in future publications.

Simulation Results

Using the aforementioned process models, the grinding circuit, shown in Figure 5(a), was first simulated using standard operating conditions found in the porphyry copper processing industry. The results from this initial simulation were then compared to the modified circuit shown in Figure 5(b). For the modified circuit, the cut sizes for the classifiers and the primary grind size were changed to best exploit the coarse particle recovery obtainable by HydroFloat™. Throughout all simulations, key performance indicators, such as mill circulating load, degree of liberation, and rougher flotation characteristics were tracked. The feed size distribution, mill capacity, and mill power were held constant for both circuits. The initial feed rate for the baseline case was set to a fixed value of 100,000 tons per day, and the specific energy of the primary grinding circuit (assuming a 27 x 41 ft ball mill) was determined to be 9.26 kW-

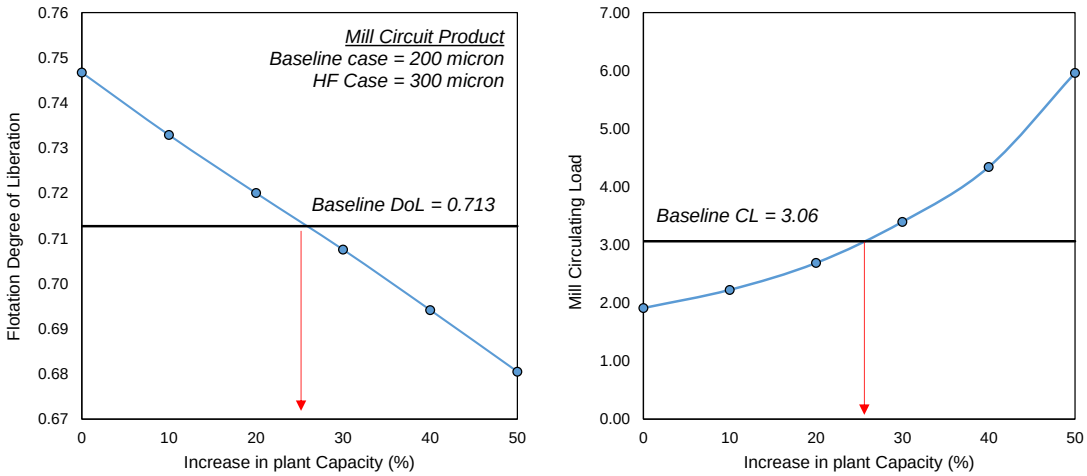

Figure 12 – Degree of liberation (left) and mill circulating load (right) for the HydroFloat™ circuit shown as a function of increased plant capacity, relative to the original circuit.

hr/ton (Wills, 2015). For the baseline case, the hydrocyclone cut point and mill capacity were adjusted until the primary grinding product (i.e. primary flotation feed) reached a P_{80} of 200 microns, with a mill circulating load of approximately 300%. Simulations with these grinding and feed parameters indicate that the degree of liberation entering the flotation circuit is 71%, and the overall rougher flotation recovery is 88% at a copper grade of 11%. Considering the feed grade of 0.58%, the tailings grade is calculated to be 0.07%.

For the HydroFloat™ circuits, the primary grinding product was increased to a P_{80} of 300 microns, and classifier cut points were then adjusted until the oversize isolated the fraction too coarse for conventional flotation (approximately 250 microns). This change in grinding size from 200 to 300 microns coupled with the rejection of coarse gangue from the HydroFloat™ produces an immediate benefit to the grinding circuit in terms of increased degree of liberation and reduced circulating load. At the baseline capacity (100,000 tons per day), the degree of liberation entering the flotation circuit increased from the standard circuit value of 71% to nearly 75%; furthermore, the mill circulating load decreased from 300% to 190%. Most notably, though, these changes were realized while maintaining an overall tailings grade (HydroFloat™ plus rougher flotation) of 0.08% Cu, only marginally higher than the 0.07% produced from the original case. The calculated rougher recovery (relative to the overall circuit feed) and grade were also similar to the original circuit performance: 87.5% Cu recovery at 11% Cu grade.

These results clearly indicate that the feed rate to the mill can be increased without sacrificing performance relative to the original circuit. To determine the "breakeven" point, new simulations were conducted at incrementally-increasing circuit throughput values, while monitoring the flotation degree of liberation and the mill circulating load. Figure 12 shows the results from these additional simulations. These values indicate that the use of the HydroFloat™ circuit can result in a 20 to 25% increase in plant capacity, without installing additional grinding equipment. This increased plant throughput may necessitate additional flotation capacity to maintain target recovery values; however, it should be noted that the implementation of the HydroFloat™ circuit actually reduced the amount of fine material entering the flotation circuit, as a result of the increased grind size and the multi-stage classification. In practice, this reduction in fines will likely produce increased recovery, as fewer particles are present in the limited flotation size range less than 10 microns.

CONCLUSIONS

The HydroFloat™ technology was specifically engineered to enable the recovery of coarse particles that were once considered to be too large to be upgraded by conventional froth flotation machines. The HydroFloat™ offers several advantages for treating coarser feeds including reduced turbulence, improved bubble-particle contacting, minimization of buoyancy restrictions, elimination of froth-pulp transfer limitations, increased particle residence time, and enhanced plug-flow separating conditions. These unique features have allowed many industrial mineral plants, such as those operating in the potash and phosphate industries, to create split-feed flotation circuits in which ultra-coarse particles lost as waste are now efficiently recovered as saleable products. More recently, potential applications of this innovative technology in the sulfide minerals industry have begun to be considered. Experimental work conducted to date using both bench- and pilot-scale test equipment indicate that the HydroFloat™ technology can successfully recover particles as coarse as 850 microns containing as little as 1% exposed sulfide mineral. Based on this capability, a split-feed circuit has been modeled and simulated to demonstrate how the HydroFloat™ technology can be used to increase the capacity of a primary grinding circuit for a hypothetical concentrator treating a typical porphyry copper ore. The circuit configuration rejects coarse well-liberated siliceous gangue that would otherwise occupy the capacity of the primary grinding mill. The simulation data demonstrate that a 20-25% increase in capacity of a concentrator may be achievable without the addition of new grinding equipment through a modest investment in new classification and flotation equipment. Due to a large potential economic return, it is recommended that a full-scale version of this concept be tested at a metal-sulfide concentrator.

REFERENCES

Ata, S., Chen, Z., & Jameson, G.J. (2009). Improving the capture of coarse particles using bubble clusters. Preprint 09-083, SME Annual Meeting & Exhibit and CMA's 111th National Western Mining Conference, Denver, Colorado.

Barbery, G. (1984). Engineering Aspects of Flotation in the Minerals Industry: Flotation Machines, Circuits and Their Simulation, in *The Scientific Basis of Flotation* (Ed: K. J. Ives), NATO Advanced Institute Services, Series E, No. 25, Martinus Nijhoff, Boston, Massatucheses, pp. 289–348.

Drzymala, J. (1994a). Characterization of materials by Hallimond Tube flotation. Part 3: Maximum size of floating and interacting particles. *International Journal of Mineral Processing, 42*, 203–218.

Drzymala, J. (1994b). Characterization of materials by Hallimond Tube flotation. Part 2: Maximum size of floating particles and contact angle. *International Journal of Mineral Processing, 4*2, 153–167.

Gaudin, A., Grob, J., & Henderson, H., (1931). Effect of particle size in flotation. *AIME Technical Publications, 414*, 3–23.

Gontijo, C., Fornasiero, D., & Ralston, J. (2007). The limits of fine and coarse particle flotation. *Canadian Journal of Chemical Engineering, 87*, 739–747.

Herbst, J.A., Rajamani, K., Lin, C.L., & Miller, J.D. (1988). Development of a multicomponent-multisize liberation model. *Minerals Engineering, 1*(2), 97–111.

King, R.P., Hatton, T.A., & Hulbert, D.G. (1974). Bubble loading during flotation. *Transactions of the Institute of Mining and Metallurgy, Section C*, 112–115.

King, R.P., & Colborn, R.P. (1971). The effect of particle size distribution on the performance of a phosphate flotation process. *Metallurgical Transactions, 2*, 354–362.

Kohmuench, J.N., Mankosa, M.J., Yan, E.S., Wyslouzil, H., & Christodoulou, L. (2010). Advances in coarse particle flotation – Industrial minerals. *Proceedings 25th International Mineral Processing Congress*, Australasian Institute of Mining and Metallurgy, Victoria, Australia, pp. 2065–2076.

Kohmuench, J.N., Thanasekaran, H., & Seaman, B. (2013). Advances in coarse particle flotation: Copper and gold. *Proceedings AusIMM MetPlant Conference*, Perth, Western Australia, 11 pp.

Laskowski, J. (1989). Frothing in Flotation, Gordon and Breach Publishers, New York, N.Y. 337 pp.

Lynch, A.J., Johnson, N.W., Manlapig, E.V., & Thorne, C.G. (1981). Mineral and Coal Flotation Circuits: Their Simulation and Control. Elsevier Publishing, Amsterdam, 291 pp.

Nageswararao, K. (1995). A generalized model for hydrocyclone classifiers. *Proceedings AusIMM, 300*(2), 21–34.

Mankosa, M.J., & Luttrell, G.H. (2001). Hindered-bed separator device and method. *U.S. Patent No. 6,264,040*. Washington, DC: U.S. Patent and Trademark Office.

Mankosa, M. J., & Kohmuench, J. N. (2003). Applications of the HydroFloat air-assisted gravity separator. In Advances in Gravity Concentration (Honaker, R.Q. and Forrest, W.R., Eds.). Littleton, CO:SME, pp. 165–178.

Mankosa, M.J., Kohmuench, J.N., Christodoulou, L., & Luttrell, G.H. (2016). Recovery of values from a porphory copper tailings stream. *Proceedings XXVIII International Mineral Processing Congress*, Québec City, QC, Paper 457, 10 pp. (in press).

Miller, J.D., Lin, C.L., Wang, Y., Mankosa, M.J., Kohmuench, J.N., & Luttrell, G.H. (2016). The significance of exposed grain surface area in coarse particle flotation of low-grade gold ore with the HydroFloat technology. *Proceedings XXVIII International Mineral Processing Congress*, Québec City, QC, Paper 455, 10 pp. (in press).

Scheludko, A., Toshev, B. V., & Bojadjiev, D.T. (1976). Attachment of particles to a liquid surface – Capillary theory of flotation. *Journal of the Chemical Society, Faraday Transactions, I*(12), 2815.

Schulze, H. J. (1984). Physico-Chemical Elementary Processes in Flotation, in Developments in Mineral Processing, Vol. 4. Amsterdam: Elsevier Publishing, pp. 238–253.

Schulze, H. J. (1977). New theoretical and experimental investigations on stability of bubble/particle aggregates in flotation: A theory on the upper particle size of floatability. *International Journal of Mineral Processing, 4*, 241–258.

Trahar, W.J., & Warren, L.J. (1976). The floatability of very fine particles – A review. *International Journal of Mineral Processing, 3*(2), 103–131.

Wills, B. A., & Napier-Munn, T. (2015). Wills' mineral processing technology: An introduction to the practical aspects of ore treatment and mineral recovery. Butterworth-Heinemann.

Yianatos, J.B., Finch, J.A., & Laplante, A.R. (1988). Selectivity in column flotation froths. *International Journal of Mineral Processing, 15*(2), 279–292.